Available online at www.sciencedirect.com

ScienceDirect

Thin Solid Films 516 (2008) 7894 – 7898

www.elsevier.com/locate/tsf

First-principles study of the electronic and optical properties of lanthanide bromide

Chenliang Li [a], Biao Wang [a,b,*], Rui Wang [c], Hai Wang [a], Zhenye Zhu [a]

[a] School of Astronautics, Harbin Institute of Technology, Harbin, China
[b] School of Physics and Engineering, and Sun Yat-sen University, Guangzhou, China
[c] Department of Applied Chemistry, Harbin Institute of Technology, Harbin, China

Received 25 March 2007; received in revised form 9 March 2008; accepted 17 March 2008
Available online 25 March 2008

Abstract

The structural, electronic and optical properties of $LaBr_3$ have been investigated using the density functional theory within generalized gradient approximation. The calculated structural parameters are in good agreement with the experimental data. The energy band structure, the density of states and atomic charges are obtained, which indicate that the covalent feature of $LaBr_3$ involves the 5*p*-orbital on La and the 4*s*-orbital on Br, and that $LaBr_3$ is an insulator with the indirect band gap. Moreover, the optical properties including the dielectric function, absorption spectrum, refractive index, extinction coefficient, reflectivity and energy-loss spectrum are all obtained and analyzed in details within the energy range up to 40 eV. And the results are compared with the available experimental data.

Keywords: Density-functional theory; $LaBr_3$; Electronic structure; Optical properties

1. Introduction

The rare-earth trihalides have been widely used in various fields such as nuclear industry, energy production and environments. The lanthanide bromide ($LaBr_3$), as a typical material of the rare-earth trihalides, is an important component of high-pressure discharge lamps and plays an essential role in the design of protection systems for cases of nuclear reactor accidents. Also $LaBr_3$ has the characteristic of intense and high-efficiency luminescence when Ce or Pr atom is doped. Due to the floppy structure of $LaBr_3$, the number of accurate experimental studies is quite limited. Sato [1] measured the optical absorption and X-ray photoemission spectra of evaporated thin films of $LaBr_3$. Kovacs et al. [2] studied the molecular structure of $LaBr_3$ by high-temperature infrared spectra. Meanwhile, Zakharov et al. [3] reinvestigated the molecular structures of $LaBr_3$ by gas-phase electron diffraction. With regard to theoretical study, it is mainly focused on the molecular properties of $LaBr_3$, including the geometric structure, vibrational frequencies, and thermochemical [4–10]. The theoretical researches referring to its electronic structure have been quite few. Adamo et al. [9,10] calculated the charges of $LaBr_3$ molecular system through the natural population analysis procedure in the framework of the natural bond orbital approach. At present, there is no theoretical report about electronic and optical properties of the bulk $LaBr_3$ using the first-principles method. However, exploring the electronic and optical properties of $LaBr_3$ should have important signification to improve the range of practical applications and elucidate the physical origin of its interesting properties.

In this work, we report a series of first-principles density function theory calculations on the structural, electronic and optical properties of $LaBr_3$. We present the optical properties, including the dielectric function, absorption spectrum, refractive index, extinction coefficient, reflectivity and energy-loss spectrum.

2. Computational method

The calculations are performed using the Full-potential Linearized Augmented Plane Wave (FP-LAPW) method based

---

* Corresponding author. School of Physics and Engineering, and Sun Yat-sen University, Guangzhou, China. Tel./fax: +86 20 84115692.
E-mail address: lichenliang1980@yahoo.com.cn (B. Wang).

0040-6090/$ - see front matter © 2008 Elsevier B.V. All rights reserved.
doi:10.1016/j.tsf.2008.03.020

on density functional theory (DFT). We used the program package WIEN2k code, and relativistic effects are taken into account within the scalar-relativistic approximation. The Perdew–Burke–Ernzerhof generalized gradient approximation (GGA) [11] was used for the exchange and correlation correction. This is due to the fact that a number of studies show that the DFT methods based on the GGA scheme can compute accurately the properties of transition metals [12–16]. The structural optimizations are conducted using the Broyden–Fletcher–Goldfarb–Shanno minimization, modified to take into account the total energy as well as the gradients. Atomic charges were calculated according to the formalism described by Segall et al. [17]. The optical properties are then calculated based on the linear response theory.

We use a parameter $R_{\mathrm{MT}}K_{\mathrm{MAX}}=8$ to control the size of basis set for the wave functions. The muffin-tin radii R_{MT} we chose are 2.5 and 2.3 for La and Br, respectively. For optical properties calculations, it is important to use a sufficient number of k points. Therefore, the changes of the optical properties with the number of k points in the optical matrix elements calculation are tested. For the sampling of the Brillouin zone, the electronic structures and optical properties used a $8\times8\times10$ and $12\times12\times12$ k-point grid generated according to the Monkhorst–Pack scheme [18], respectively.

The optical properties of $LaBr_3$ is determined by the frequency-dependent dielectric function $\varepsilon(\omega)=\varepsilon_1(\omega)+i\varepsilon_2(\omega)$ that is mainly connected with the electronic structures. The imaginary part $\varepsilon_2(\omega)$ of the dielectric function $\varepsilon(\omega)$ is calculated from the momentum matrix elements between the occupied and unoccupied within selection rules. The real part $\varepsilon_1(\omega)$ of the dielectric function $\varepsilon(\omega)$ can be derived from the imaginary part $\varepsilon_2(\omega)$ using the Kramers–Kronig dispersion equation. And all other optical constants, such as the absorption spectrum, refractive index and reflectivity can be derived from $\varepsilon_1(\omega)$ and $\varepsilon_2(\omega)$ [19].

3. Structure determination

$LaBr_3$ is hexagonal (the space group is $P6_3/m$) with a bimolecular unit cell. Lanthanide and bromide occupy 2a in (1/3, 2/3, 1/4) and 6h in (0.385, 0.299, 1/4) sites, respectively [20]. The crystal structure is optimized by force and energy minimization. In the process of optimization, all atoms are moved towards their equilibrium positions. The experimental and calculated lattice parameters are summarized in Table 1. The a and c lattice constants are overestimated by 1.6% and 2.3% comparing with the experiment results, respectively. These deviations are within the admitted range of the errors of the first-principles methods. Thus, our structure is in reasonable agreement with the experiment.

Table 1
Crystal structures of $LaBr_3$

		$a=b$ (Å)	c (Å)	V (Å^3)
$LaBr_3$	Experiment [a]	7.951	4.501	246.424
	Calculation [b]	8.082	4.605	258.797

[a] Ref. [20].

[b] This work.

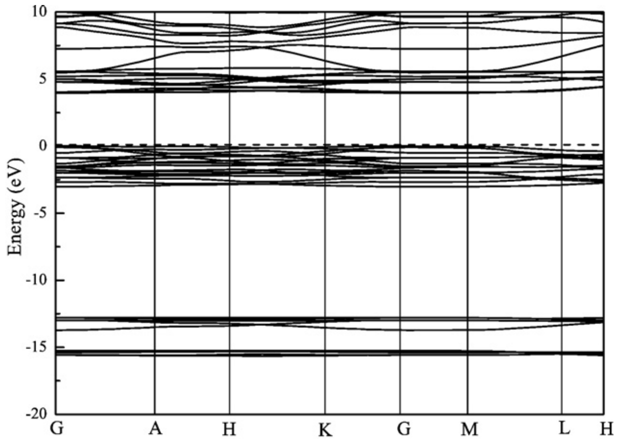

Fig. 1. Calculated energy band structure of $LaBr_3$ crystal.

4. Electronic properties

In the following, we calculated the electronic structures of $LaBr_3$ at the equilibrium structure. The energy band structure and density of states (DOS) are shown in Figs. 1 and 2, respectively. The energy band structure is calculated along the way that contains the highest number of high-symmetry points of the Brillouin zone, namely G→A→H→K→G→M→L→H.

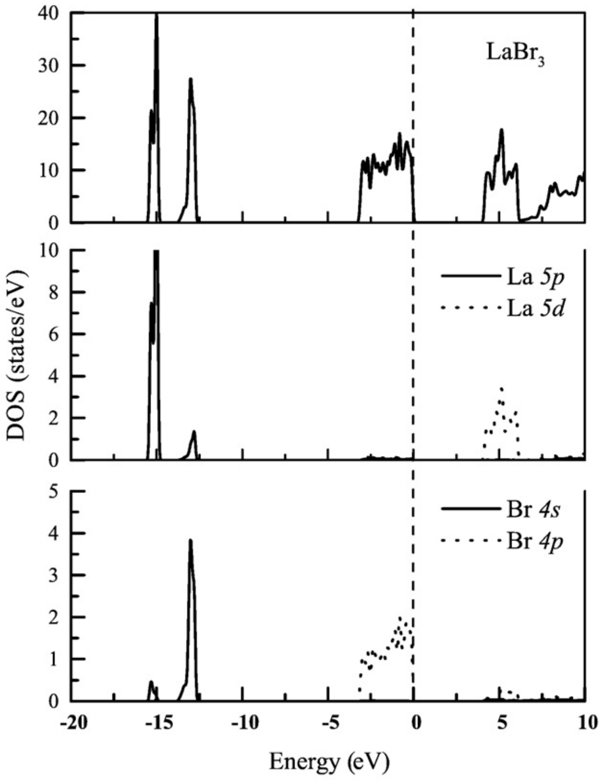

Fig. 2. Calculated density of states of $LaBr_3$ crystal.

The zero energy is arbitrarily taken at the Fermi level (dashed line).

The top of valence band (VB) and the bottom of conduction band (CB) is at the point M (0, 0.5, 0) and G (0, 0, 0), respectively. Thus, $LaBr_3$ has an indirect band gap of 3.75 eV. Unfortunately, no experimental and theoretical information about the value of the band gap is available for $LaBr_3$ at present stage. The band gaps predicted by DFT are smaller than the experimental data, which means that our result underestimates the real band gap of $LaBr_3$. In our calculation, the scissors operator on both the electronic structure and the optical properties were not considered. The lowest bands around −32.8 eV (not shown in Fig. 2) consist of 5*s* state of La. The La 5*p* state is located at around −16.2 eV. The bands around −13.2 eV are derived from the 4*s* state of Br. The highest occupied valence band consists of 4*p* states of Br that decide the top of the valence band. The lowest unoccupied conduction band consists of 5*d* states of La that decide the bottom of the conduction band. By analyzing partial density of states, there is a well known hybridization between Br 4*s* and La 5*p* orbitals. Therefore, we can conclude that $LaBr_3$ has also some covalent features in spite of its main ionic character. This result is consistent with other theoretical computations [8,9].

We also calculated the atomic charges for $LaBr_3$ because it is a good method to understand bonding behavior. The atomic charges results are given in Table 2. The charge transfer from La to Br is about 0.6 electrons. Therefore, we concluded that the bonding behavior of $LaBr_3$ is a combination of covalent and ionic nature. The result is consistent with our DOS calculation.

5. Optical properties

Based on the electronic structure, the dielectric functions of $LaBr_3$ are calculated. And the $\varepsilon_2(\omega)$ and $\varepsilon_1(\omega)$ as a function of the photon energy are shown in Fig. 3. The imaginary part $\varepsilon_2(\omega)$ of the dielectric function is directly connected with the energy band structure. The threshold peak of the imaginary part appears at about 3.82 eV that is related to the direct transition from the top of valence band to the bottom of conduction band at the M point. Peak A at about 9.87 eV corresponds to the transition from Br 4*p* VB to La 5*d* CB, and peaks B (15.08 eV) and C (24.34 eV) are ascribed to the transition of inner electron excitation from La 5*p* and Br 4*s* VB to CB. For the real part $\varepsilon_1(\omega)$, it presents four main peaks at 7.32 eV, 8.56 eV, 13.22 eV and 23.46 eV, respectively. And it reduces to a minimum at 26.28 eV.

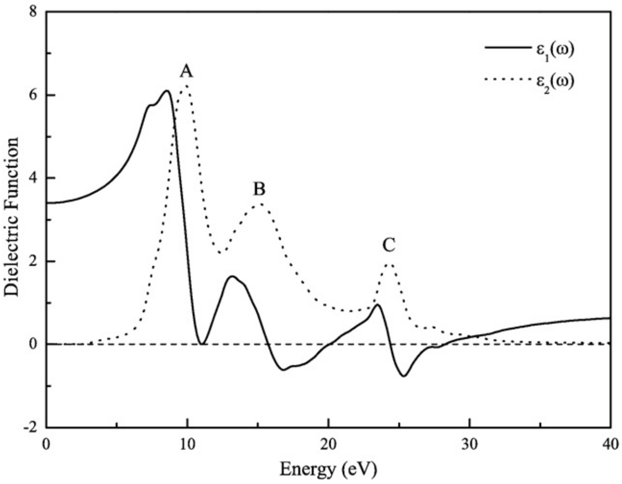

Fig. 3. Calculated imaginary part $\varepsilon_2(\omega)$ and real part $\varepsilon_1(\omega)$ of the dielectric function $\varepsilon(\omega)$ for $LaBr_3$ crystal.

Fig. 4(a)–(e) shows the calculated results on the absorption spectrum, refractive index, extinction coefficient, reflectivity and energy-loss spectrum, respectively. It can be seen that the calculated absorption spectrum is in good agreement with the experimental data [1]. But the intensity obtained in the experiment and our calculation is somewhat different. For example, the peak at 25.04 eV is stronger than the experimental value. For the discrepancy, one could arise from the use of evaporated thin film of $LaBr_3$ in the experiment. The other could be the broadening of the experimental and theoretical curves. The degree of such broadening can influence the intensity of the peak [21], but it is not given in the experiment. In our calculation, we used Gaussian smearing which is 0.4 eV. The absorption spectrum starts at 4.06 eV. In the range from 0 to 4.06 eV, the reflectivity is lower than 15%, which indicates that $LaBr_3$ material is transmitting for frequencies less than 4.06 eV. Moreover, when the frequency is higher than 30.77 eV, the material becomes transparent. The energy-loss spectrum describes the energy loss of a fast electron traveling the material, and its sharp peak is usually associated with the plasma energy [22]. The energy-loss spectrum of $LaBr_3$ presents four prominent peaks which are consistent to the roots of $\varepsilon_1(\omega)$. At present, there are not yet any experimental results on these optical constants except absorption spectrum. Therefore, we hope that our calculated results could serve as a reference for future experimental study.

Table 2
Atomic charges of $LaBr_3$

Species	*s*	*p*	*d*	Total	Charge (electron)
La	2.40	6.61	1.39	10.40	0.60
Br (1)	1.84	5.36	0	7.20	−0.20
Br (2)	1.84	5.36	0	7.20	−0.20
Br (3)	1.84	5.36	0	7.20	−0.20

6. Conclusions

In summary, we calculate the crystal structure, the band structure, density of states, atomic charges and optical properties for $LaBr_3$ by means of the density functional theory within the GGA. Our structural parameters are in good agreement with the experimental data. $LaBr_3$ is an insulator with an indirect band gap that is 3.75 eV. And the top of the valence band is decided by 4*p* states of Br and the bottom of the conduction band is decided by 5*d* states of La. Further, $LaBr_3$ has covalent characters. In the end, based on the electronic band structure, the dielectric function, absorption spectrum, refractive index,

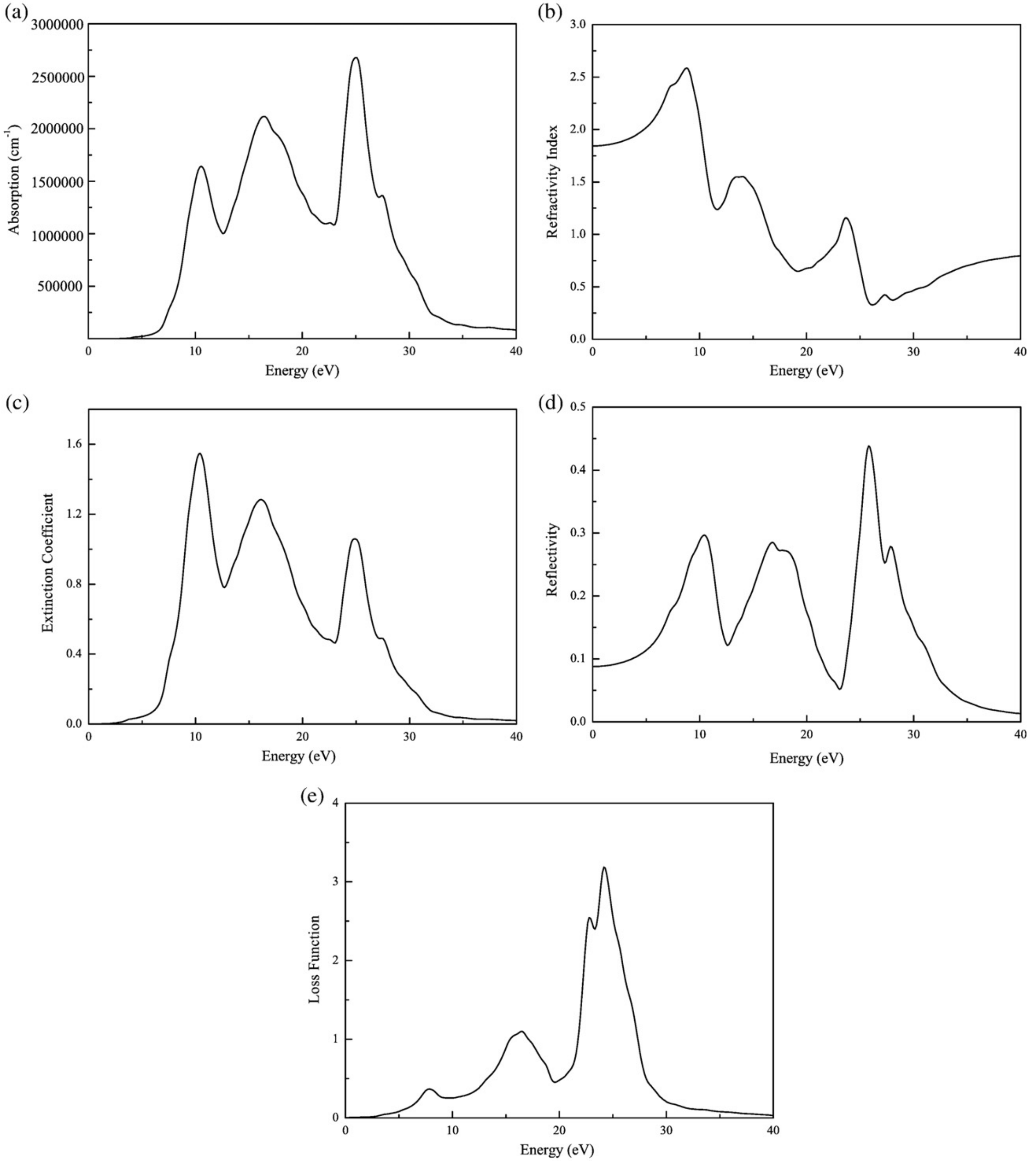

Fig. 4. Calculated optical constants of $LaBr_3$ crystal: (a) Absorption spectrum, (b) refractive index, (c) extinction coefficient, (d) reflectivity, and (e) energy-loss spectrum.

extinction coefficient, reflectivity and energy-loss spectrum are obtained. The relations of the optical properties to the interband transitions are also discussed in detail.

Acknowledgment

This work was supported by the National Natural Science Foundation of China (10572155, 10172030, 50232030) and The Science Foundation of Guangdong Province (2005A10602002).

References

[1] S. Sato, J. Phys. Soc. Jpn. 41 (1976) 913.
[2] A. Kovacs, R.J.M. Konings, S. Booij, Chem. Phys. Lett. 268 (1997) 207.
[3] A.V. Zakharov, N. Vogt, S.A. Shlykov, N.I. Giricheva, I.E. Galanin, J. Mol. Struct. 707 (2004) 147.
[4] A. Kovacs, Chem. Phys. Lett. 319 (2000) 238.
[5] C. Adamo, V. Barone, J. Comput. Chem. 21 (2000) 1153.
[6] V.G. Solomonik, O.Yu. Marochko, Zh. Fiz. Khim. 74 (2000) 2296.
[7] V. Vetere, C. Adamo, P. Maldivi, Chem. Phys. Lett. 325 (2000) 99.

[8] M. Dlog, H. Stoll, H. Preuss, J. Mol. Struct. (Theochem) 235 (1991) 67.
[9] C. Adamo, P. Maldivi, Chem. Phys. Lett. 268 (1997) 61.
[10] C. Adamo, P. Maldivi, J. Phys. Chem. A 102 (1998) 6812.
[11] J.P. Perdew, K. Burke, M. Ernzerhof, Phys. Rev. Lett. 77 (1996) 3865.
[12] C. Adamo, P. Maldivi, J. Phys. Chem. A 102 (1998) 6812.
[13] V. Jonas, W.J. Thiel, J. Chem. Phys. 102 (1995) 8474.
[14] L.A. Eriksson, L.G.M. Pettersson, P.E.M. Siegbahn, U.J. Wahlgren, J. Chem. Phys. 110 (1995) 872.
[15] M. Castro, D.R. Salahub, R. Fournier, J. Chem. Phys. 100 (1994) 8233.
[16] B. Delly, M. Wrinn, H.P. Luthi, J. Chem. Phys. 100 (1994) 5785.
[17] M.D. Segall, C.J. Pickard, R. Shah, M.C. Payne, Mol. Phys. 89 (1996) 571.
[18] H.J. Monkhorst, J.D. Pack, Phys. Rev. B 13 (1976) 5188.
[19] S. Saha, T.P. Sinha, Phys. Rev. B 62 (2000) 8828.
[20] K. Kramer, T. Schleld, M. Schulze, W. Urland, G. Meyer, Z. Anorg. Allg. Chem. 575 (1989) 61.
[21] N.V. Skorodumova, R. Ahuja, S.I. Simak, A. Abrikosov, B. Johansson, B.I. Lundqvist, Phys. Rev. B 64 (2001) 115108.
[22] Z.W. Chen, M.Y. Lv, L.X. Li, Q. Wang, X.Y. Zhang, R.P. Liu, Thin Solid Films 515 (2006) 2433.